Induced Drag Reduction using Multiple Winglets, looking beyond the Prandtl-Munk Linear Model

U. La Roche* and H.L. La Roche†
La Roche Consulting, Zuerich, Switzerland, CH-8053

Abstract

A redefinition **of multiple winglet configurations is proposed in order to understand and facilitate exploiting the massive induced drag reductions of streamwise staggered multiple winglets, which, using the Prandtl-Munk vortex sheet model are not predicted. Multiple winglets are either staggered streamwise (feathered wingtips) or have no such stagger (Cone tip boxes, endplates and other classic configurations). This contribution considers the fact, that we have on the one hand well understood and replicated winglet systems (no stagger) which are rendered with sufficient accuracy by the Prandtl-Munk model of a fixed vortex sheet in streamwise direction, free of drag, neglecting rolling up. On the other hand selected cases new and old, such as the Spiroid, Split-Wing or the Winggrid are being reported which exhibit streamwise staggered winglets and where the experimental results point to much smaller induced drag than predicted with the Prandtl-Munk linear model. The paper shows, how taking into account a grid effect of staggered multiple winglets on the deflected massflow of a wing system within linear models. The actual gap for conceptual understanding and calculating between experiment and prediction by linear models is bridged to a new perspective beyond the linear Prandtl-Munk model. Out of this new perspective follows a reassessment of selected multiple winglet configurations with superior performance potential.**

Nomenclature

c.	=	center of lift, gravity, etc.
alfa_nom	=	angle of attack at MCR01 test
AR	=	aspect-ratio
b	=	span
b'	=	effective span, separation of rolled up tip vortex pair
c	=	chord
c_{avg}	=	average chord of wing
c_{blade}	=	chord of winglet or blade
C_{D0}	=	drag coefficient excluding induced drag
C_D	=	drag coefficient
C_L	=	lift-coefficient
Cl_0	=	Cl at center of wing
Cl_{avg}	=	average Cl of wing
Cl_{calc}	=	Cl derived by using slope of lift curve
d	=	distance along free stream PIV
delta_alfa	=	error between 2-D calculation and measurement
delta_e	=	added massflow (winglets)
dp_b	=	static pressure differential pressure to suction side of Winggrid
dp_{ch}	=	static pressure differential blade in channels
dz	=	vertical distance for PIV
e	=	span efficiency, induced drag elliptic wing / induced drag compared wing. No viscous polar effects included

* Dr. sc. Techn. Owner, La Roche Consulting, Heilighuesli 18, CH-8053 Zuerich, member
† Dr. sc. Techn., La Roche Consulting, Heilighuesli 18, Ch-8053 Zuerich, non-member

e_{tot} = resultant span efficiency from massflow and effective span
$e_{formfactor}$ = effective span/effective span elliptic
k = quadratic drag term in C_D: k * C_L ^2
h = vertical extension of wingtips
L = half span
L/D = lift vs drag
L2 = span of multiple winglets
LE, TE = leading and trailing edge of a profile or grid
M = Mach number
m = deflected massflow per span
n = number of blades
o_v = ratio of blade chord divided by separation (LE to LE) of blades = c/t
Re = Reynolds number
R_k = radius of rankine vortex core
t = separation LE to LE of blades
v = freestream velocity
w = down velocity in wake
x = coordinate along free stream PIV
y = span coordinate
z = vertical coordinate
β = Prandtl linearizing factor for compressible flow
δ = stagger angle
ε = grid deflection angle (Betz)
γ = free stream incidence angle relative line connecting LE's of Winggrid blades
κ = kappa Betz grid correction factor

I. Introduction

Experimental results for multiple winglet configurations are reported, which, using the Prandtl-Munk[1] vortex sheet model are not predictable. To understand why, multiple winglets are separated in two different classes, they are either staggered streamwise (feathered wingtips) or have no such stagger (tip boxes, endplates and other classic configurations). Cases new and old, such as the Spiroid[2], Split-Wing[3] or the Winggrid[4] are being reported which exhibit streamwise staggered winglets and where the experimental results point to much smaller induced drag than predicted with the Prandtl-Munk linear model (see sample configurations summary page 9).

In addition if we use this linear model in the latter cases for calculation of the lift of the winglets, the measured lift distributions on the individual winglets are not reproduced by far, in contrast to the case of classic wingtip configurations with no streamwise stagger of winglets. For predicting the performance of multiple staggered winglets ways and means have still to be found, which overcome the unability of the linearized Prandtl-Munk model to render the additional effect streamwise staggered winglets have.

Specialised CFD solvers, which include simulation of the nearfield force-free vortex sheets including their rollup as shown by Smith[3] for the Split-Wing appear to make a difference.

His results point to the existence of Non-Munk wingtip configurations: multiple winglets which are staggered streamwise along the chord of the main wing and for which the impact on induced drag is not visible using the classic linear models. From an analysis of the massflow model for the Winggrid an extension to LINAIR PRO[5] (or similar programs) is found, that allows precalculation of such Non-Munk wingtip configurations to acceptable accuracy. The linear Prandtl-Munk model does not replicate all effects of streamwise stagger of winglets. With the interpretation of staggered winglets as (turbine)-grids the additional deflected massflow of such a grid in the expression for the span efficiency is accounted for. Using this extension with selected outputs from LINAIR PRO an overview on multiple winglet wingtips is obtained, which is quantitatively consistent with experiment, from Split-Wing to Winggrid and including well known configurations such as the Spillman[6] wingtip.

For benchmarking of the wing systems discussed we use the span efficiency e, which is derived from the relative induced drag for a given lift comparing an optimum elliptic wing to the wing system concerned.

We use the span efficiency defined as excluding viscous drag polar effects, eq.(1).

$$e = \text{induced drag of elliptic planform reference wing} / \text{induced drag of wing system} \quad (1)$$

Spreiter & Sacks[7] have shown, making no assumptions on the geometric topology of the wing systems analysed, but including rollup of vortex sheet, that there appear only two parameters for the benchmark figure e

$$e = f(b'/b, Rk) \tag{2}$$

Their analysis for eq. (2) identifies the effective span b' , the asymptotic separation of the rolled up tip vortices and the thickness of the (Rankine) vortex core 2*Rk, to define e. Their analysis however does not show the existence of a minimum limit of induced drag (respectively a maximum of e) as postulated by the Prandtl-Munk model. In making the extension for e.g. LINAIR PRO it is found that the span efficiency e can be written as consisting of two contributions, one from the effective span and one from the deflected mass flow. This extension results in an easy to use prediction tool including effects of streamwise stagger of multiple winglets, allowing to look beyond the Prandtl-Munk linearized model and establishing thereby a tool for benchmarking the results of experimental tests and related CFD procedures.

The appendix gives an updated overview on the available experimental evidence for the Winggrid as reference background. New results confirming the control line model tests are reported using inpendent PIV measurements (particle image velocimetry) of one of the actual test wings.

II. Models for representing wing systems

Prandtl [8], Munk [1], later Cone [9] and modern authors as Kroo [10] treating classic wing systems confirm, that in essence it is possible to increase e substantially above 1.0, the value of the optimum planform elliptic wing.

If we look into the background of such classic wing systems, we find that e is calculated to close approximation by the calculus of velocity potential across the vortex sheet leaving, as demonstrated by Cone using electrical analog models. For results in line with reality, the wing systems under study must not have streamwise staggered winglets. Such stagger has no additional effect on the resultant span efficiency in the linearized Prandtl-Munk model used, contrary to results from experiment or more refined CFD calculus. Also lift distributions for the individual staggered winglets are in error. But total and element forces (in the case of multiple winglets the sum of lift contributions) are rendered still close to reality. A modern treatment of different configurations within classic wing systems based on an essentially linear models is due to Kroo, demonstrating the C-wing with e=1.5 as a near practical maximum in this class.

Cone did include in his survey multiple winglet configurations. Comparing his results to measured results with multiple winglet cofigurations having streamwise staggered positions of the winglets, we find strong disagreement between prediction and experiment. His survey by an electric analogy calculation was clearly based on the linear Prandtl-Munk model, which calulates staggered winglets as if no streamwise stagger would be present or would have any impact on the outcome.

Including wings with multiple winglets which are staggered streamwise and rendering this effect in CFD appears as an important extension of wing systems vs classic systems above.

With multiple staggered winglets added to a base wing we find at the outer part, where the multiple winglets are attached, a branching of the vortex sheets leaving the wing system staggered at different chord positions. The proposed condition of no stagger (or no effect of this stagger) at branching per vortex sheet along span leaving (Prandtl-munk vortex sheet model) appears not any more to be an applicable model.

Examples for such more general wing systems are e.g. the multiple fanned winglet wingtip with dihedral angles between the winglets such as the famous wingtip by John Spillman [6], the Spiroid [2] , the Split-Wing[3] or finally the fanned multiple wingtip with parallel blades, the Winggrid[4] .

Usually such configurations were analysed first by experimental procedures as reported for the Spiroid and the Winggrid before trying to understand them.

It is found, that e can get still further above 1.0, surpassing wing systems with no staggered branching of vortex sheets (e.g. the C-wing) by a wide margin.

However test results with wingtips with fanned dihedral and non-parallel staggered winglets in the past, not explained by the calculation with a linear model, were often silently dismissed. Also the reported results for e did not materially challenge the basic assumption, that still classic wing systems calculus using the linearized Prandtl-Munk model would cover also those cases.

As was demonstrated by Smith for the case of the Split-Wing, calculating the e value for systems with streamwise staggered winglets requires consideration of the interaction of the staggered vortex sheet systems in the nearfield. To us it appears, that the investigation of Smith was not, as perceived by many experts in the field, only a clarification on some minor nonlinearities in special wingtips for more accuracy. In essence it has opened the vision to the treatment of wing systems, which for fundamental reasons are not describable by the basic Prandtl-Munk vortex sheet model, because their streamwise stagger of winglets produces effects which the linearized model does negate, precisely because of the Munk stagger theorem .

The Split-Wing analysed by Smith did show an increase of e of some 11% in experiment and free force vortex sheet CFD (which translates to 11% reduction of induced drag), about 6% more than calulated using the linear Prandtl-Munk model. This is still a small first indication towards the experimental evidence of a fanned, streamwise staggered multiple wingtips with parallel blades showing an increase of the span efficiency e to values well beyond 2 for Winggrid configurations.

New models or extensions of the most widely used Prandtl-Munk model to represent streamwise staggered winglets would facilitate the design of these configurations. Starting with the pionieering work of Smith we see as a possible solution the use of highly sophisticated CFD procedures (e.g. with wake relaxation for obtaining true free-force vortex wakes), which appear to need however very careful application control, as failed students projects along these lines for a Winggrid demonstrate at present. So if we could just get a practical extension to routines as e.g. LINAIR PRO, even at the cost of precision, this would represent a wellcome step forward for the preliminary design and benchmarking of such systems by experiment and new CFD calculation methods alike.

This is the idea of the next chapter, analysing the Winggrid configuration and generalising the findings for application to streamwise staggered multiple winglets.

III. Winggrid insights

At the center of our own experimental investigations was and still is the fanned multiple wingtip with parallel blades (Winggrid, cf. Fig. 6), which due to its near rectangular spanload allows a simple and sufficiently accurate model for understanding the span efficiency e.

With near rectangular spanload we find near 2-D flow independent of span location, which allows for straightforward procedures for analysis and design. The Winggrid configuration is used as working model for a general analysis of e.g. the Split-Wing and the Spillman wingtip in order to asses the performance of wing systems showing a streamwise staggered branching of the vortex sheets leaving at the tip but not having parallel winglet blades.

The Winggrid shows three typical phenomena of such staggered multiple wingtips.

A. Critical stagger angle (rotation angle of grid plane from plane of main wing).

From the test data available for a fullscale aircraft with Winggrid blade force measurements it can be concluded, that the flow through a Winggrid behaves like the flow through a finite row of turbomachinery blading.

If the stagger angle δ is smaller than a critical angle depending on design angle of attack, the free flow through the grid of fanned winglets is blocked, we call this cutoff. The arrangement then is working like an ordinary slit wing. With free flow through the grid we observe, that each blade contributes its individual deflected massflow. Below is a short explanation on how to calculate this cutoff condition, cf. figure 1.

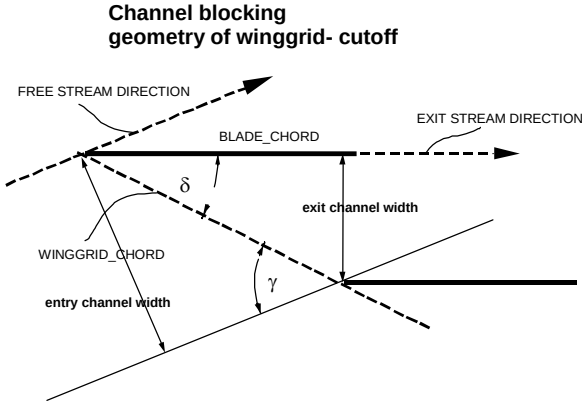

Figure 1: Bernoulli model for blocking at cutoff

The static pressure difference from entry freestream condition to channel exit is given , eq. (3) by the channel contraction defined by the streamlines as (Bernoulli):

$$dp_{ch} = -1 + \left[\sin(\gamma) / \sin(\delta) \right]^2 \qquad (3)$$

The corresponding pressure differential for the flow around the Winggrid is approximated and averaged over Winggrid chord by the lift as, eq. (4):

$$dp_b = 2 \cdot \pi \cdot \gamma \qquad (4)$$

From the condition for full exit flow through the Winggrid slit spaces between the blades we can infer the necessary stagger angle $\delta = f(\gamma, dp_{ch} < dp_b)$. (Experiment shows, that dp_b has a maximum limit around dpb < 1.5 in Cp units).

For higher subsonic Mach numbers we observe that the linearised Prandtl factor β for compressible flow is identical for dp_b(lift) and dp_{ch}(channel between blades), that is for velocity and streamline disturbances due to compressibility[11]. So the cutoff condition for full volume flow from exit of channels between blades of a Winggrid, eq. (5):

$$dp_b/dp_{ch} >= 1 \qquad (5)$$

is invariant for M < 1 within applicability of the Prandtl factor β.

For a general fanned winglet configuration this condition for stagger angle δ bigger than the critical stagger angle in order to avoid cutoff varies with the span coordinate y along the winglet grid.

B. Overlap.

Decreasing the ratio of blade chord to blade separation, the overlap o_v, decreases flow deflection as shown by ordinary turbine grid theory (Betz grid theory[12]). If the winglets or blades are not parallel, then the overlap will vary along span of the winglets and result in variable flow deflection. Overlap is the parameter that decides the steepness of the lift distribution among the winglets, low overlap (high (t/c)) will result in a flat distribution of individual blade lift load. The lift distribution calculus used for the Winggrid is based on rectangular spanload, which results in 2-D flow and permits a simple calculation using representation of the blades by their circulation.

Finding the individual loads is then solving the quadratic matrix (n blades) of the mutual interference of these circulations. The overlap enters the respective diagonal matrix coefficients (details for this blade load calculus to be found in the *working paper*‡ on our webpage).

For a general fanned and streamwise staggered winglet system with the blades not parallel, only the sum of individual winglet loads is rendered with some credibility by using a linear model (Prandtl-Munk). Exact calculation would require a CFD procedure capable of rendering the nearfield vortex wake rollup.

C. Deflected massflow and the Betz coefficient κ

κ *as function of (t/c)*: The additional deflected massflow of a streamwise staggered grid is (n-1) times the rectangle, as illustrated in figure 2 for the case of Winggrid below cutoff.

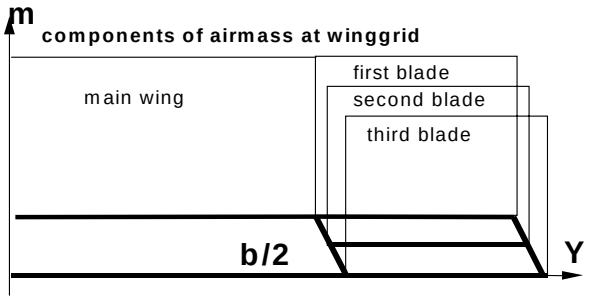

Figure 2: deflected mass flow model Winggrid

For a general case not having rectangular span load the additional deflected mass is approximated by (n-1) * airmass of the winglet part span.

The deflected massflow is not the resulting lift, it indicates over what massflow the generation of lift is distributed, therefore more deflected massflow for the identical lift results in less induced drag.

In the example of the figure below we assume three parallel winglet blades.

With rectangular spanload each blade generates 1/3 of lift/span, with a contribution to induced drag by 1/9, the square of lift. With three blades the total contribution is then 1/3, one third because of three times deflected massflow and total lift per span unit identical to main wing.

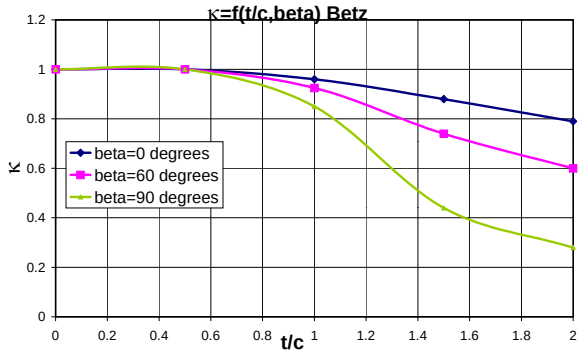

Figure 3: dependence of deflection κ on (t/c) (Betz)

Deflected massflow is proportional to the effective deflection given by e.g. the Betz coefficient κ(overlap), overlap=c/t, cf. figure 3. It should be noted, that in a grid of multiple winglets the resulting deflection is not only a function of the angle of attack on the winglet, but in addition of the grid parameter o_v. (We observe, that even for o_v = 0.5 or t/c = 2 the deflection in a grid is lowered from κ = 0.95 to κ = 0.8; in ordinary LINAIR PRO calculus the lift on the blade would be reduced to 50% taking Cl*c as a measure.)

For a general case with fanned multiple winglets κ and t/c are variables of the span coordinate, and consequently the deflected mass per span unit is given by the factor κ * (t/c).

‡ La Roche, U. and L.,and To, F., "A Fanned Winglet Wingtip with parallel blades, Fluid Dynamics and Design", working paper 02, URL: http://www.Winggrid.ch/research.htm, [cited 8 March 2004]

Summary of insights

topic		*generalising for non-parallel winglets*
Cutoff	section A	critical stagger angle a function of span coordinate
Overlap	section B	lift distribution on winglets depending on o_v not rendered by linear model, which renders only sum of winglet loads
Deflected massflow added	section C	(n-1) times contribution at span y
Lift	section B	Sum of individual lift of winglets in grid

IV. Deflected massflow and effective span for staggered multiple winglets with LINAIR PRO and Betz grid approximation

The span efficiency e for a wing system may be conceptualised as the product of two different components, one connected to the effective span and another due to the deflected massflow of the wing momentum model.

A. Special case Winggrid

For the easy understandable Winggrid configuration with near rectangular spanload distribution, this conceptualisation lends itself to a simple interpretation of the socalled „massflow formula“ for the span efficiency, eq. (6):

$$e = (1+L2/L*(n-1))*4/\pi = (1 + delta\_e) * e_{formfactor} \quad (6)$$

- The deflected massflow (1+delta_e), e.g. is increased by multiple winglets. This contribution will after Spreiter & Sacks define the radius of the rolled up tip vortex core. The expression (1+L2/L*(n-1)) is the sum of different contributions to the deflected massflow, namely 1 the rectangle over span, L2/L *(n-1) the additions caused by the additional winglets with n winglets and in the case of the Winggrid with rectangular spanload over the parallel winglets span.
- The effective span is defined as the separation of the rolled up tip vortex pair. Here $4/\pi$ is the increase in effective span for a rectangular spanload compared to the elliptic reference wing spanload distribution.

In a Winggrid (parallel winglets or blades) with constant slope of lift curve along span the Winggrid part must be adjusted (stretched) by a factor $1/\kappa$ (kappa Betz grid theory), with $\kappa((t/c))$ the coefficient giving net deflection for given angle of attack with a grid of spacing t and blades having chord c. Note that the resulting lift forces are not directly dependent on the chord of the blades, smaller blade chords will result in higher local Cl , steeper lift distribution along the Winggrid and a reduced κ for the winglet blades in grid configuration.

B. General multiple winglet case

In a most general case with winglets not parallel and variable chord along their span, twist included, the deflected mass contribution for dy of span at a given span y (along the winglet) may be expressed as, eq. (7):

$$L2/L * (n-1) * \kappa(y) * sum(Cl*c(y)/c_{avg})/L2/Cl_{avg}*dy \quad (7)$$

with $\kappa(t/c)$ the Betz deflection coefficient and (t/c)=1/ov=f(y) and dy the increment span. t is the separation LE to LE of the winglets and c their chord. $sum(Cl*c(y)_n/c_{avg})$ is the sum of the n winglet lift forces at point y of the total winglet configuration.

In order to use LINAIR PRO for calculation of forces needed in eq. (7) the geometry data have to be prepared to reflect the grid effect. For winglets in a grid the local angle of attack must be multiplied with a factor (κ * (t/c)), where κ gives the falloff of deflection with increasing (t/c) and (t/c) reflects that in a grid the local lift coefficient is (t/c) times the grid lift. After this corrections are made LINAIR PRO or equivalent gets the forces including the grid effect of the multiple winglets.

The infinitesimal contribution at span coordinate y has to be normalized with Cl_{avg} in order to add it up correctly with the contribution of the main wing part, so we get the final expression as, eq. (8):

$$Delta\_e_{massflow} = \int_{winglet\text{-}span} (L2/L * (n-1) * \kappa(y) * sum(Cl*c(y)/c_{avg})/Cl_{avg}/L2*dy) \quad (8)$$

The effective span b' is defined (Betz[16]) as the separation of the c.g. of vorticity leaving the wing system. For elliptic spanload distribution this is exactly b * π / 4. In order to calculate it for general cases the expression has to be numerically solved based on the actual spanload distribution. Within our approximation we use the

simplified expression, which is exact for elliptic and rectangular spanload and a useful approximation for convex distributions of spanload vs span in between, eq. (9):

$$b'/b = Cl_{avg}/Cl\_0 \quad (9)$$

with Cl_0 the lift coefficient at center of wing system. Relative to the elliptic reference case this gets us, eq. (10):

$$e_{formfactor} = b'/b'elliptic = Cl_{avg}/Cl\_0/\pi*4 \quad (10)$$

and finally the total span efficiency as product of the two contributions, eq.(11)

$$e_{tot} = e_{formfactor} * (1 + Delta\_e_{massflow}) \quad (11)$$

Note on using using LINAIR PRO for multiple winglets:

Weissinger calculus based on the linear Prandtl-Munk model with vortex sheet leaving in freestream direction, neglected rollup and free of drag, does not image the effect of streamwise staggered winglets on deflected massflow. This appears to be a consequence of the Munk stagger theorem. So for configurations outside restricted classic applications like wing systems describable by lifting lines, a linear model renders only integral lift forces and related lift coefficients realistically, individual lift distributions on winglets prove to be unreliable (as can be shown for the lift distribution on the winglets with Winggrid). For full representation of the effects of a grid of staggered multiple winglets we have to add the grid effect on the element forces using e.g. the Betz grid approximation explained above.

Therefore we are using for approximation of staggered multiple winglets a restricted selection, e.g. of the LINAIR PRO outputs only:

total forces,element forces, $sum(Cl*c)_{winglet\_span}$ and Cl_0 and Cl_{avg} in the expressions above.

Cl_{avg} follows from total force, Cl_0 the lift coefficient in the center of the wing system taken from the lift distribution $Cl*c/c_{avg}$ of the total configuration.

C. Sample calculation LINAIR PRO extended with Betz grid approximation

Here we follow step by step the extension of e.g. LINAIR PRO which was used for compiling the quantitative overview on winglet configurations given in the next chapter (example is Spillman with 3 winglets as patented). After adjustement of the local angles of attack on the winglets with the factor (κ * t/c), the configuration is ready for calculation of the data including grid effect.

Step 1:

Do a calculation for the configuration e.g. with LINAIR PRO
Needed OUTPUTS #1 to #5 used are:

#1:

!Configuration Forces & Moments
!Case alpha beta Mach CL CD CY CM CR CN e

#2: output LINAIR PRO whole configuration

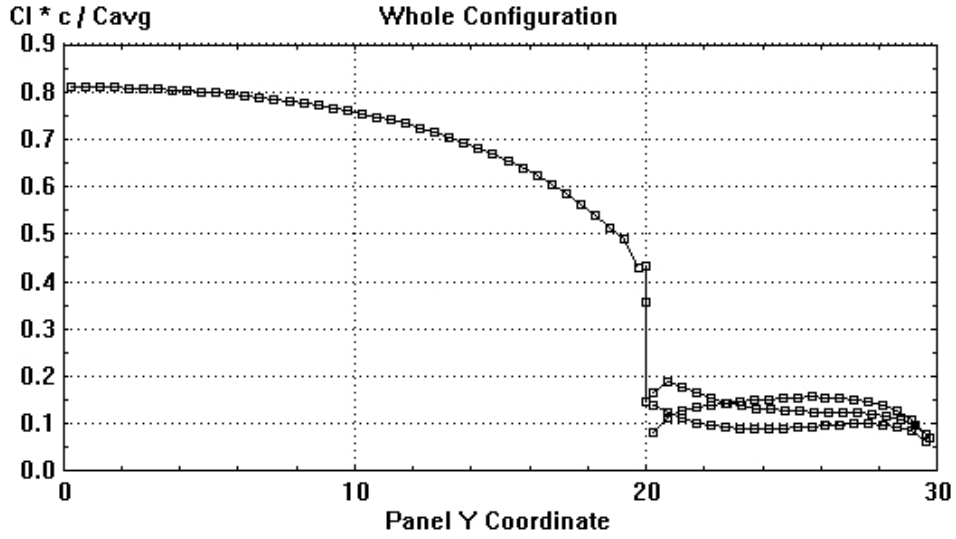

#3: output LINAIR PRO element 1, main wing

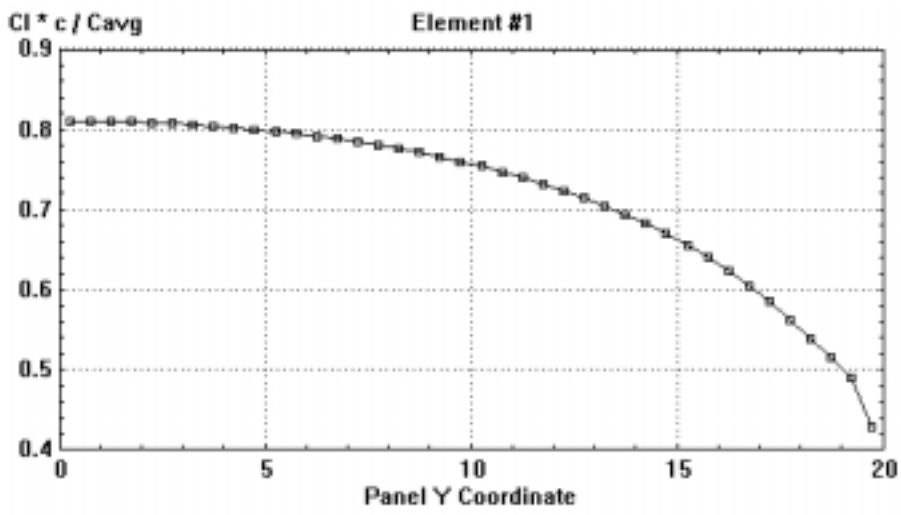

#4:

Cl_0/Cl_{avg}=0.81/0.597=1.355, $e_{formfactor}$ = (4/π)/1.355 = 0.94 (effective span subelliptical)

#5:

Lift distribution of all the winglet elements:

!Element #4

! X	Y	Z	Cl*c*q/(cavg*q0)	Cl
6.02187	20.24620	0.95659	0.19015	0.33548

Step 2:

Transfer the files to excel sheet for calcuation of delta_e (additional massflow) and $e_{formfactor}$ (resulting effective span)

The added deflected massflow per span increment dy at span coordinate y is calculated after the Winggrid model inserting the local total lift Cl*c(y)/c_{avg} as, eq. (12) and (8):

L2/L * (n-1) * κ(y) * sum(Cl*c(y)/c_{avg}/L2/Cl_{avg}), with κ(t/c) the Betz deflection coefficient and (t/c)=f(y) (12)

Step 3:

Analyse the configuration in LINAIR PRO format for cutoff condition along winglet span and correct in the excel sheet the delta_e value (no contribution to added deflected massflow in cutoff)

if angle of attack > stagger angle * 1.5 then cutoff (no contribution of span element)

Step 4:

Take final corrected values from excel sheet for sum(delta_e) and $e_{formfactor}$ to calculate the span efficiency attack as, eq. (13), (11):

$$e = (1 + e\_delta) * e_{formfactor} \quad (13)$$

Note on restriction of definition streamwise staggered

The experimentally checked range of streamwise stagger treated here is:

Stagger is >= chord length of winglet at root of multiple winglet configuration. Configurations inside the interval 0 < stagger < 1 (chord length) are not considered, their treatment is not supported by the simplified extended Betz LINAIR PRO in full and is furthermore not of interest as borne out by our first experimental survey using an asymmetric model airplane wing in 1992, mostly due to excessive cutoff at o_v > 1.

V. Summary of results for reference multiple wingtip configurations, calculated with LINAIR PRO plus Betz grid approximation (reference cases in frame)

(angle of attack 10 degrees, Split-Wing 9 and 5 degrees)

Configuration	rel_tip_span L2/L rel_tip_height h/b	e calc by LINAIR PRO, extended with Betz grid approximation	Theory & experiment	e from LINAIR PRO	Image LINAIR PRO
Classic single wingtip	h/b = .32 L2 negligible along span	contributions: delta_e = .40 b' eff span = 1.11	n.a.	1.56 exact, (not a multiple staggered wingtip)	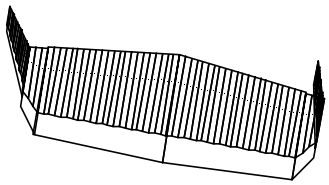
Split-wing	L2/L = .33 h/b negligible	1.10 for 9 deg and 1.13 for 5 deg (cutoff at winglet root for 10% of blade span at 9 deg angle of attack)	1.09 to 1.13 Smith Calc with special CFD and experiment	1.06	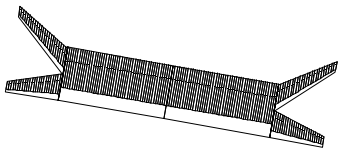
Cone tip boxes	h/b = 0.2 L2/L = .33	contributions: delta_e = .10 b' eff span = 1.26	n.a.	1.39 exact (not a multiple staggered wingtip)	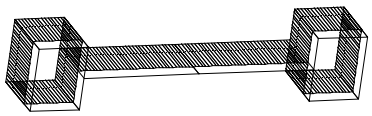
Winggrid107 control-line model endplate small effect revealed in experiment	L2/L = .25 (h/b = .09 necessary for cutoff at Clmax = 1.5)	1.89	1.91 calc massflow winggrid experiment 1.9-2.1+	0.8	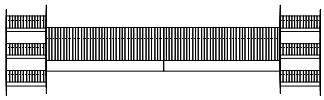
Winggrid Prometheus fullscale endplate neglible effect	L2/L = .17 (h/b = .025 for cutoff at Clmax = 0.7)	1.99	1.92 calc massflow winggrid experiment 2.0	0.9	
Spillman_patent (twisted blades with negative angle of attack)	L2/L = .33 h/b = .05	1.36 due to neg attack at root no cutoff	n.a.	.83 (for small angles near zero)	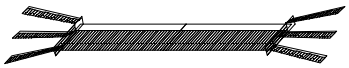
Spiroid_triangle Cutoff up to 30% blade span from blade root closing loop negligible effect	L2/L = .33 h/b = .1	(1.46 without cutoff) with cutoff 1.33	n.a.	1.17	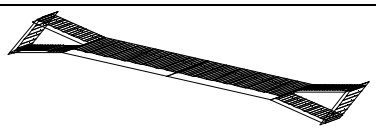
Spiroid_rectangle closing loop negligible effect	L2/L = .33 h/b = .1	1.73	1.69 calc massflow winggrid	1.4 for small angles a bit less	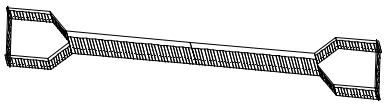

Note:

Only multiple winglet configurations with essentially rectangular spanload can be corrected for constant slope of the lift curve over wing span by applying the Betz correction on the effective chord of the (Winggrid, rectangle Spiroid). Spillman type or fanned dihedral winglets will show different slope of lift curve for main wing and multi-winglet wingtip span and will therefore be only optimal at a fixed angle of attack.

A. How span efficiency e for multiple, streamwise staggered winglet wingtips is obtained using LINAIR PRO and the Betz grid approximation:

The resultant span efficiency e is obtained by considering added deflected massflow and increase of effective span due to a multiple winglet arrangement, eq. (14), (11):

$$e = (e(\text{elliptic}) + \text{delta\_e}) * e_{formfactor}(\text{spanload distribution}) \quad (14)$$

where delta_e is added deflected massflow normalized to Cl_{avg} of the respective configuration. If cutoff is present (e.g.at the root base of the blades for fanned winglet tips), no contribution to the deflected massflow takes place. For elliptic spanload distribution the $e_{formfactor} = 1$, for rectangular we have $e_{formfactor} = 4/\pi$.

The $e_{formfactor}$, representing the spanload distribution is taken from LINAIR PRO output and represents in physical terms an approximation of the influence of spanload distribution on the separation of the rolled up vortices (effective wing span).

The resultant span efficiency is thereafter the product of the individual contributions from added massflow delta_e and changed $e_{formfactor}$.

For the calculation of the additional deflected massflow only the contributions along the fanned winglets are to be summed, where no cutoff takes place. The cutoff is evaluated using the information available from Winggrid tests and theoretical models (see working paper footnote page 5).

The example of the classic single wingtip configuration shows using the method in reverse, starting from the span efficiency e given by LINAIR PRO to find the separate contributions of increased deflected massflow delta_e and increase in effective span b‘.

Example:

A $e_{formfactor}$ of 1.0 represents elliptic spanload with effective wing span = $\pi/4$ * b

A $e_{formfactor}$ of 1.27 represents rectangular spanload with effective wing span = b (ideal case of Winggrid).

The procedure for calculating span efficiency for multiple winglet configurations is a three step procedure:

STEP	*OPERATION*	*RESULT*
#1 lift distribution for configuration corrected for inclusion of grid effect	LINAIR PRO calculate lift distribution with parameter wake= -0.1 (wake follows freestream direction)	Cl*c over span and for the winglets Cl_0 and Cl_{avg} for $e_{formfactor}$
#2 deflected massflow	additional deflected massflow from $Cl*c/c_{avg}$ of winglets and κ-Betz = f((t/c))	delta_e = f(n)
#3 corrections for cutoff	subtract span elements of added massflow where cutoff is incurred	added massflow delta_e corrected for cutoff $e = (1 + \text{delta\_e}) * e_{formfactor}$

B. Reference cases for calibrating and checking the method used are:

- Split-Wing (Smith, NASA TP 3598, 1996)
- Winggrid107 (experimental proof with control line model 2003 and PIV TU Linz 2003/2004, reference footnotes on pages 14,15)
- Winggrid of fullscale testbed PROMETHEUS (tests idaflieg99[15] and Mollis97[13])
- Classic single wingtip and tip box wing (Cone) (LINAIR PRO renders exact value e, which is after our method analysed for the contributions on increase in deflected massflow delta_e and increase in effective span b‘) .

The cases for Spiroid and Spillman variants are analoguous cases based on the basic three step procedure checked with the reference cases above.

They show, that basically the Spiroid is not essentially different from the Winggrid and that well known multiple winglet configurations as e.g. proposed by J. Spillman do in fact a nice job, if configured not to exploit a tip vortex flow for gaining additional forward thrust, but similar to Winggrid for gaining additional deflected massflow and an increased $e_{formfactor}$ (increased effective span). However if the multiple winglets are not parallel, several potential advantages are lost:

- It is not any more possible to correct the fanned multiple winglet wingtip for identical slope of the lift curve compared to the base wing.
- Due to fan out the deflected additional massflow is strongly reduced towards tip
- More complicated compressibility effects in high subsonic speeds are to be expected near winglets root

The cases listed do show practically identical results with and without endplates, for the Winggrid this has been verified experimentally also, a Spiroid configuration is from these results expected not to need closed loops (as patented) to work.

C. Assumptions:

- LINAIR PRO as other methods based on the Prandtl-Munk linear vortex sheet model do deliver useful results for configuration forces even for cases, that do not fit the model, such as streamwise staggered winglets. The configuration (angle of attack of the winglets) is before calculation corrected to reflect the multiple winglets flow deflection including the Betz grid effect by the factor $\kappa * t/c$
- The Betz grid theory (or equivalents) gives the resultant deflection of a (infinite) grid of blades in function of the blade separation. In application of the results to multiple winglets no substantial correction for a grid consisting of just a few blades is necessary. The added deflected massflow for span dy at span coordinate y is calculated after the Winggrid model inserting the local total lift $Cl*C(y)/c_{avg}$ as

$$L2/L * (n-1) * \kappa(y) * \text{sum}(Cl*c(y)/c_{avg})/L2/Cl_{av}*dy \quad (15)$$

  with $\kappa((t/c))$ the Betz deflection coefficient and (t/c)=f(y) and eq. (7)
- For single wingtip configurations, or multiple winglets having no streamwise stagger, LINAIR PRO delivers correct values for lift distributions and the span efficiency
- The conditions for cutoff found with the Winggrid apply also to fanned multiple winglets (with special consideration of the winglets root part and dihedral angles)

The method incorporating the results of Betz grid theory for quantitative assessment of the addition in deflected massflow by multiple winglets is applicable for cases of streamwise staggered winglets only, since as even the case of the Split-Wing showed, cutoff by near overlapping winglets is a severe restriction. This limitation was also evident from the experimental prescreening tests with asymmetric aircraft models in 1992.

We think the approximation method combining element force values from e.g. LINAIR PRO with deflected mass flow calculus using Betz grid theory described above does show acceptable error for purpose of preliminary design (better than a few % in span efficiency for cases with e > 1.5), at least for the cases selected and in perspective of the rather simple tools and routines used (e.g. LINAIR PRO and Excel).

D. Conclusion:

At present we know of two CFD based procedures to represent in a realistic way multiple and streamwise staggered winglet configurations.

- A high precision approach was demonstrated by S. Smith in NASA TP 3589. The results for the Split-Wing configuration tested in parallel experimentally were obtained by calculating the true force free vortex sheets leaving the wing, including partial rollup, in the nearfield a few chord lengths downstream using iterative wake relaxation. Induced drag was obtained using the classic Trefftz plane integration.
- A working approximation is found, using basically LINAIR PRO for getting the forces on the wing configuration elements (including grid influence). Interpreting the fanned winglets as a true (turbine) grid, the additional deflected massflow delta_e using the Betz grid deflection coefficient κ with the grids t/c is calculated. From the ratio Cl_avg/Cl_0*4/π the $e_{formfactor}$ (effective span) is approximated. The total span efficiency then is obtained by the product, eq. (11):

$$e_{tot} = (1 + \text{delta\_e}) * e_{formfactor} \quad (16)$$

  As the tests with the Split-Wing and the Winggrid did show, this simplified routine works well to a limited precision (a few % error) still acceptable for design and benchmarking purpose.

VI. Addendum on experimental test results:

A chronological overview of selected experimental evidence for the Winggrid configuration is added, which constitutes the basis of the assertion, that staggered multiple winglets show different and in general higher span efficiency e than the Prandtl-Munk model for the same wing system is able to explain.

A. 93/94 windtunnel tests Winggrid, reported in ICAS Sorrento96[4]

Due to low Re >= 40'000 on the actual blade of the parallel blades wingtip (named Winggrid) these tests showed only 30% to 50% of expected effect on induced drag evaluated with the slope of C_L^2 vs C_D compared

to slope of elliptic reference wing. The example shows a two blade Winggrid with high and low stagger angle

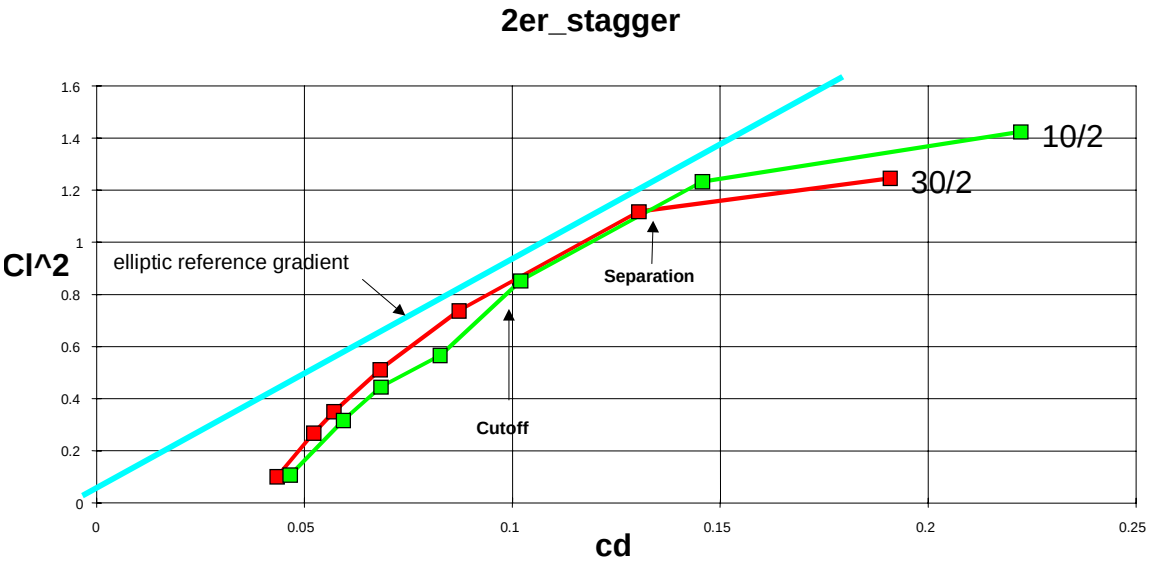

Figure 4: polars windtunnel test 93/94, 10/2 is a Winggrid with stagger angle 10 degrees 2 winglets

with Cutoff at Cl<0.9 against the elliptic reference gradient of Cl^2 vs C_D, cf. figure 4

The expected effect was precalculated based on the postulated massflow model of a multiple fanned wingtip with parallel blades below cutoff (no viscous polar drag effects accounted for).

Over the span of the winglets we have in this case constant massflow and total lift per span unit equal to main wing, deflection angle according to lift distribution over the winglets. In the Sorrento paper a heuristic formula was used, which was later rectified to the physical model on the basis of the detailed winglet load measurements in the PROGRID tests Mollis 97, see ICAS Melbourne98[13], an updated treatment for the calculation of e is found in the *working paper Fluid Dynamics and Design* ‡ (footnote page 5).

A typical test result does show a maximum lift coefficient, where the Winggrid changes to behaviour as a simple slit wing, we call this the cutoff. At still higher lift coefficient separation starts.

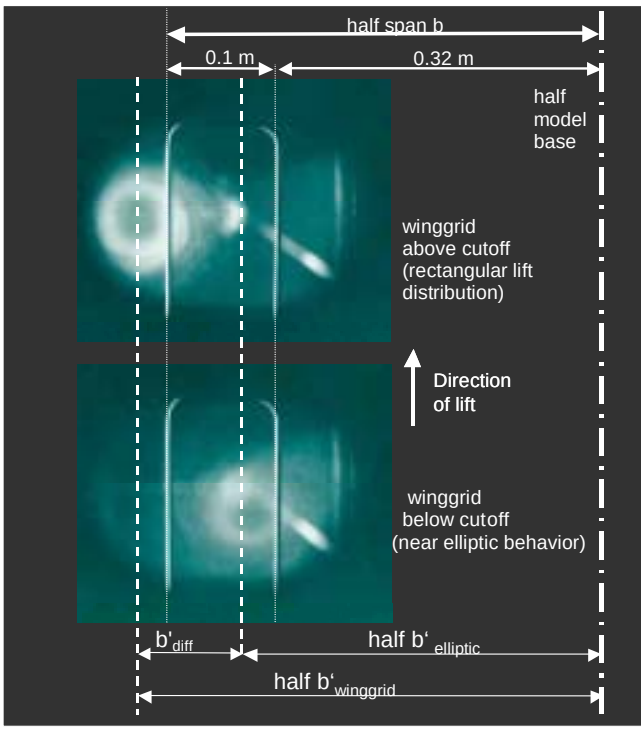

Figure 5: check location rolled up vortex windtunnel tests 93/94, impact of cutoff

As reported in the Sorrento[4] paper, polar test runs were checked by concurrent test of the location of the rolled up vortex downstream in the windtunnel and by testing concurrently the c. of lift on the halfmodel used deduced from the balance measurements for the half wing models used, cf. figure 5. Winggrid above and below cutoff shows a marked difference in effective half span b'_{diff} .

B. Prometheus fullscale tests

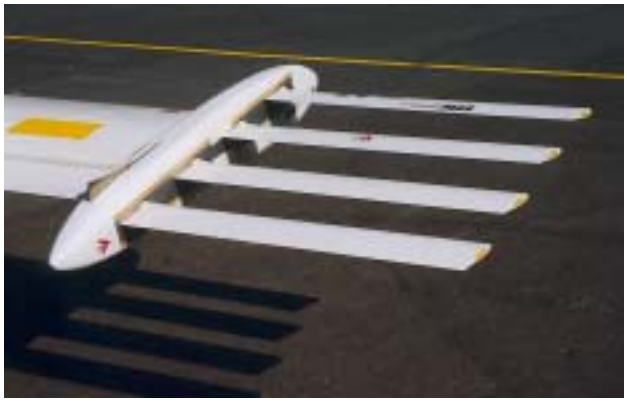

Figure 6: Winggrid used on fullscale testbed 97/99, main profile HQ 44/ 14.5 at Re > 2e6, Winggrid blade profile Selig 2027 at Re >0.5e6

These exploratory tests were followed by a first full-scale test with Re on the blades > 500'000 in 1997 (ICAS Melbourne98[13]), including winglet load data and verified by independent measurements 1999 idaflieg, (CEAS Potsdam00[14]). The experimental results obtained confirm, that near rectangular spanloads with span-efficiencies e > 2 are produced, cf. figure 6.

The idaflieg99[14, 15] test compared two configurations with identical fuselage; elliptic sailplane wing with span 23 m and rectangular test wing span 12 m with 17% halfspan Winggrid. The evaluations based on drag polar were complemented by visualisation of the tip vortex structure using smoke bombs, indicating a strong change of vortex structure for the Winggrid wingtip, cf. figure 7.

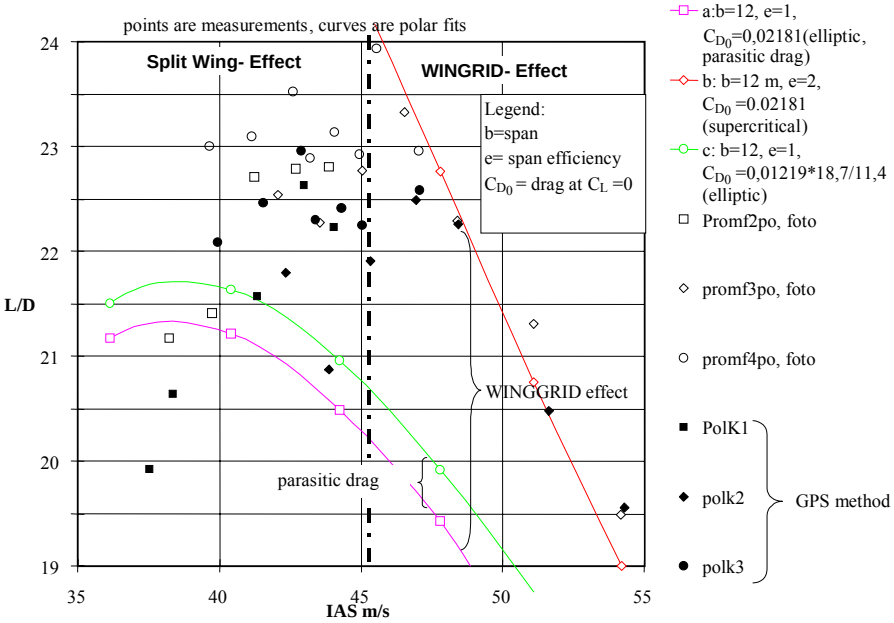

Figure 7: idaflieg99 PROGRID polar, foto is photographic idaflieg method

Fourteen points define the quadratic polar for the Winggrid configuration above IAS 45 m/s. the maximum L/D shown at L/D =24 is not the polar maximum given by equal contributions of induced drag and friction drag, it is the maximum resulting at the IAS where cutoff is gradually setting in, see the points to the left of the cutoff limit IAS = 45 m/s (this cutoff speed is set by the tested Winggrid configuration, it is a design parameter that can be appropriately choosen).

Besides confirming a span efficieny e = 2 above cutoff setting in at IAS 45 m/s from polar gradient, the direct comparison made it possible to evaluate the amount of additional interference drag caused by the test Winggrid. The parasitic drag was obtained by comparing C_{D0} for the 23 m sailplane wing and the 12 m Winggrid wing by elimination of the common fuselage drag. The Winggrid effect measured is reduced by the parasitic drag present (mostly interference drag of endplates and Winggrid blades). As verified, the amount of parasitic drag present corresponds to the interference drag on the Winggrid endplates caused by the 4 blades and the junction of main wing to Winggrid as executed in the test specimen.

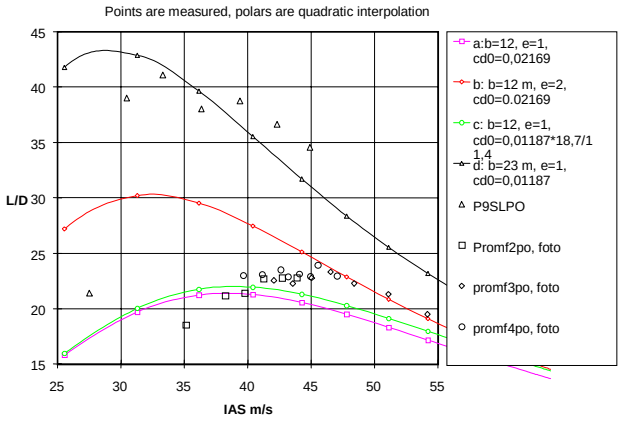

Figure 8: overview polars idaflieg99

The amount of parasitic drag for the idaflieg99 PROGRID fullscale test configuration used was not minimized in the actual design used, the target of these tests was verification of rectangular spanload and span efficiency e at high enough Re (low values of the quadratic drag term k). Optimizing of parasitic drag as carried out for the MCR01 prototype with Re > 200'000 for c_{blade} suggests this parasitic drag to be around 5%-8% of C_{D0} of the wing without Winggrid tip.

Figure 8 is a recapitulation of the polars measured and calculated. Measured polars are for the 23m span sailplane L/D max at 43 and the 12m span Winggrid wing with extrapolated L/D max at 30, but L/D max measured at 24 at cutoff.

In addition to the polar measurements there were taken pictures for visualisation of the Winggrid tip vortex development, cf. figure 9. The result point to a quite different tip vortex than resulting from an elliptic wing.

Figure 9: parallel trails for b'=b

The selected picture shows the near parallel tip vortices caused by rectangular span load.

C. MCR01 prototype

In 2001 we had for a few days testing cooperation with DYNAERO in checking their prototype MCR01 with experimental Winggrid, cf. figure 10. For getting the aircraft ready for subsequent tests our job was to check and adjust the Winggrid to working status. After correcting the blade angles of attack by iteration of flights with blade load measurements a status of rectangular spanload was attained. Here we just report the check on error limits of measured and calculated blade loads.

From the calculated and measured lift distributions we did calculate the resultant angles of attack using as independent inputs :

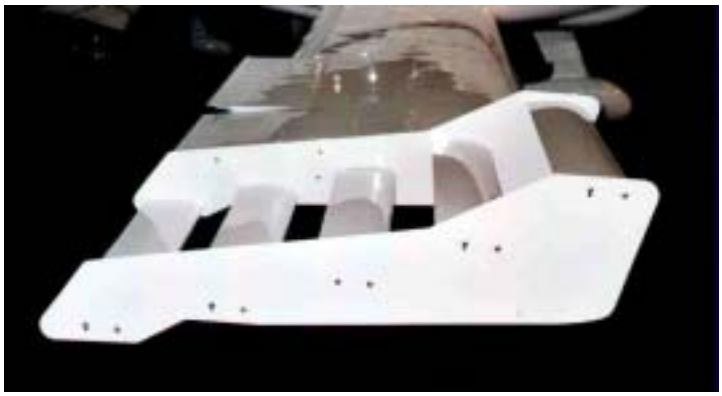

Figure 10: Winggrid of MCR01 prototype motorglider

- Total load and individual blade loads as measured by straingauges
- Speed IAS
- Aircraft weigth and geometric data
- Lift distribution as calculated, assuming rectangular spanload and using adjusted calculation parameters for the blade angles of attack
- Target load of Winggrid for 100% rectangular spanload

Because the geometric angles of attack of the blades were not known from start, we did carefully iterate the effective values by using the lift distribution calculus with the measured lift distribution as input and looking for the corresponding individual angles of attack of all the five blades.

A final check on the total accuracy of load measurement and lift distribution calculus accrues from the check of the formula for angle of attack, comprising effects of residual angle of attack (due to Betz correction error)

and additional angle of attack due to torsional flexure of the wing due to the specific Cm-value of the Winggrid in function of its load distribution. This formula was, eq. (17):

$$\text{Delta\_alfa} = \text{alfa\_nom} * \text{rel\_load} + k1 + k2 * \text{rel\_load} - \text{alfa\_avg} \quad (17)$$

Delta_alfa	error
Alfa_nom	mean angle of attack for 100% Winggrid load calculated
Alfa_avg	mean angle of attack for Winggrid load measured
Rel_load	measured load/100% load calculated
K1	bias or residual angle of attack (e.g. const = -0.33)
K2	angle of attack caused by wing torsion (e.g. const = 0.25)

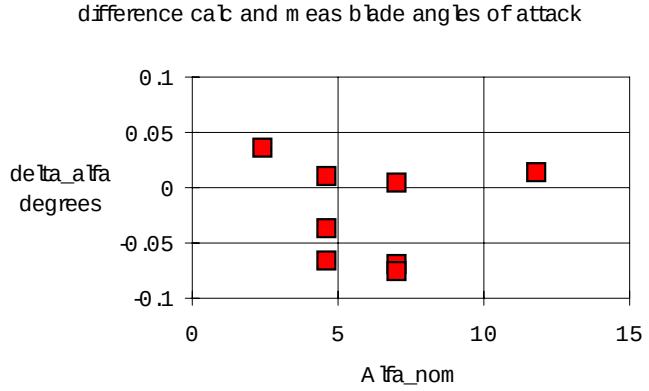

The error is < 0.1 degrees, which among other conclusions confirms, that we attained rectangular spanload, this being the key assumption of the calculus used, q.e.d.,cf. figure 11.

K1 checks Betz correction. Since its value is just a fraction of a degree, it can be concluded, that the Betz correction for equal slope of the lift curve for main wing and Winggrid is very nearly at correct settings and wing torsion was neglible.

Figure 11: errors of angle of attack compared to 2-D vortex matrix calculation

D. Control line model

From recent tests 2002/2003[§] with a control-line model at Re around 50‘000 on the blades we had again clear confirmation of Winggrid performance, a typical test summary is shown below:

Span efficiency e, cf. table 1, shows variation due to different configurations and blade profiles. (It is found using a quadratic polar including in e viscous effects, this explains the range of span efficiencies shown for different main wing profiles). Measured maximum lift coefficients of the Winggrid configurations near or in stall were found to be about 40% greater than with the elliptic configuration.

Variable ranges	Winggrid configuration	Elliptic wing configiuration	unit
Lift coefficient Cl	0.7-1.8	0.7-1.3	-
Velocity V	9-15	11-16	m/s
Parameters			
Model mass	2.76	2.72	kg
Span (including Winggrid)	1.07	1.07	m
Wing reference area S_{ref}	0.2675	0.2675	m^2
Winggrid span fractionL2/L	.33	n.a.	-
Profile main wing	NACA 8511		chord 0.25 m
Profile Winggrid blades	thickness < 7%		chord 0.085 m
Resulting Polar coefficients			
Span efficiency e	**1.3 to 2.2**	**0.95-1**	**-**
Zero lift drag coefficient Cd0	**0.19-.23**	**0.18-.2**	**-**
Maximum lift coefficient Cl_{max}	**1.5 - 1.8**	**1.1-1.3**	**-**

Table 12: Parameters and measured ranges of variables for Winggrid configuration.

[§]La Roche Consulting, ”test report: replication of winggrid effect at low Re number”, URL: http://www.Winggrid.ch/current.htm, [cited 8 March 2004]

Figure 13: control-line model for low Re tests

Background:

A control-line model, instrumented and flying in the open, provides the test environment for flying in free air as shown below, cf. figure 13. The model is either flown with rectangular wingtips (called "elliptic" configuration) or with exchangable Winggrid wingtips. Evaluation in table 12. was done with a quadratic polar interpolation of test data, including viscous drag polar effects in the span efficiency e. The quadratic viscous drag term k was controlled by wing profile designs, cf. table 12 above. (see range of span efficiencies measured without correction for k), cf. figure 14.

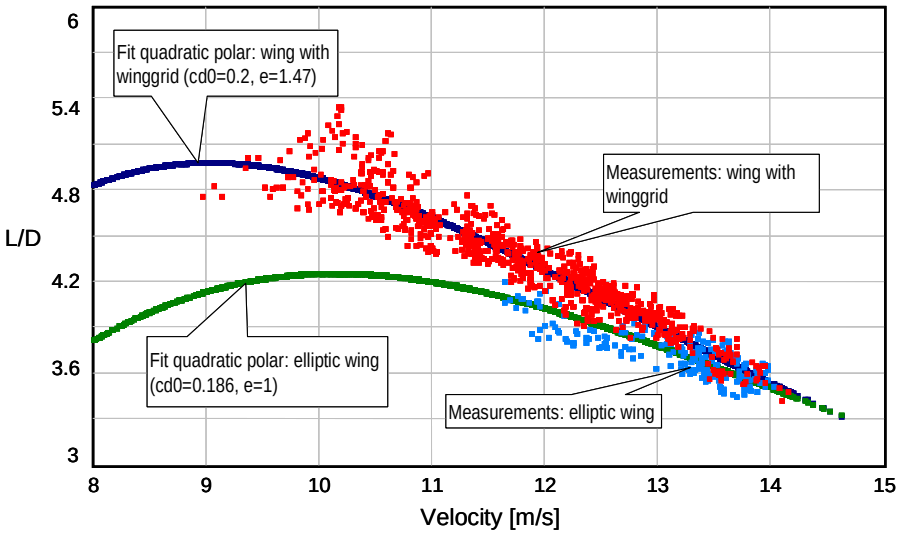

Figure 14: polars from control-line model tests 2002/2003

E. PIV-Tests of control line model wing configurations

For the actual wing with Winggrid, cf. figure 15, a PIV (particle image velocimetry) measurement of the tip vortices was done independently at the TNF University Linz 2003/2004[¶] . The results on the downward displacement velocity of the respective tip vortices confirmes our own polars measurements with the control line model setup.

Figure 15: control line model wing for PIV tests

The results obtained are also consistent with the LINAIR PRO calculations using the Betz grid extension, treated in this paper above.

At the Institute for Fluid Dynamics of the Johannes Kepler University, Linz, Austria the sample test series was executed by Peter Wimmer.

[¶] La Roche Consulting, "PIV tests of control line model wing configurations", URL: http://www.Winggrid.ch/current.htm, [cited 8 March 2004]

The PIV (particle image velocimetry) setup does take double images at fixed distances behind the wing sled, which moves at a constant velocity through still air in a wide tunnel.

The velocity choosen of 10 m/s fits into the speed range of the control line model of 8 to 16 m/s. Pictures were taken at 0.2, 0.3 and 2.2 m behind TE of the wing. The identical configurations tested with the control line model were used, *rect* being the wing with rectangular endpieces for the elliptic case e=1 and *grid* is the wing with Winggrid with a verified e=2.1+ in the control line tests (which within testing precisision is also the value calculated with the deflected massflow model for the Winggrid geometry used).

We conclude twofold confirmation of the Winggrid behaviour expected,cf. figures 16,17:

- Whereas for *rect* the transverse separation of the rolling up vortices is asymptotically diminishing, the equivalent locii of the vortex centers for *grid* remain at essentially constant separation (as required for near rectangular span load).
- A simple and concluding evidence for the value of the span efficiencies accrued using the expressions for the downward velocity w of the vortex centers for grid and rect for comparing. In retrospective PIV could be an instrumental method for directly measuring the span efficiency e with exclusion of any profile drag influences (no separations), because the downward velocity w is only dependend on the free stream velocity v, the lift coefficent Cl, the aspect ratio AR and the span efficiency e. Spreiter & Sacks show these downward velocities of the vortex centers to be given by the expressions, eq. (18):

$$w/v = -0.41 * Cl / (\pi * AR * e);\ \text{elliptic } e = 1 \qquad (18)$$

For grid $Cl = Cl_{calc}$ (Cl_{calc} = alfa * 2 * π, alfa net angle of attack of wing)
For rect $Cl = Cl_{calc} * AR / (AR + 2)$

The vortex sheet in the center has a downward velocity of, eq. (19):

$$w/v = -2 * Cl / (\pi * AR * e) \qquad (19)$$

This latter formula follows directly from consideration of the deflected mass model (expressed by the span efficiency e) and elliptic spanload distribution. In this summary we have replaced AR in the original formula of Spreiter & Sacks for elliptic spanload by the expression AR * e for Winggrid rectangular spanload in order to check the experimental evidence. Apart from numerical corrections due to differences of vortex separation b', such an extension is supported by the derivation of the vortex vertical speed by Spreiter & Sacks: the vertical speed is dependent on the force exerted by the wing expressed in downwash w. For the same lift a higher e means lower w.

See also A. Betz[16] on behaviour of vortex systems.

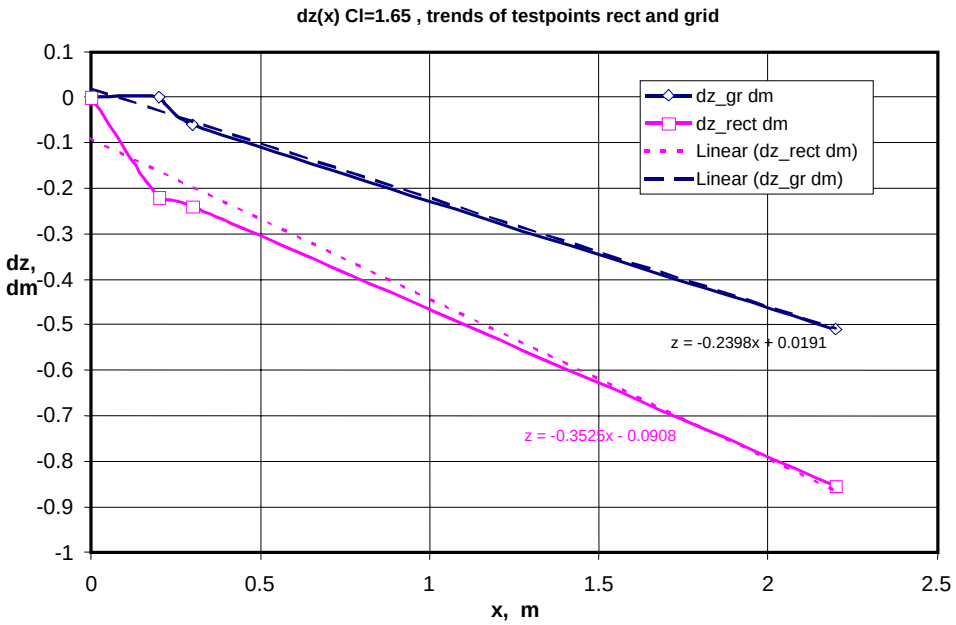

Figure 16: testdata PIV for vertical displacement of *grid* and *rect* vortices.

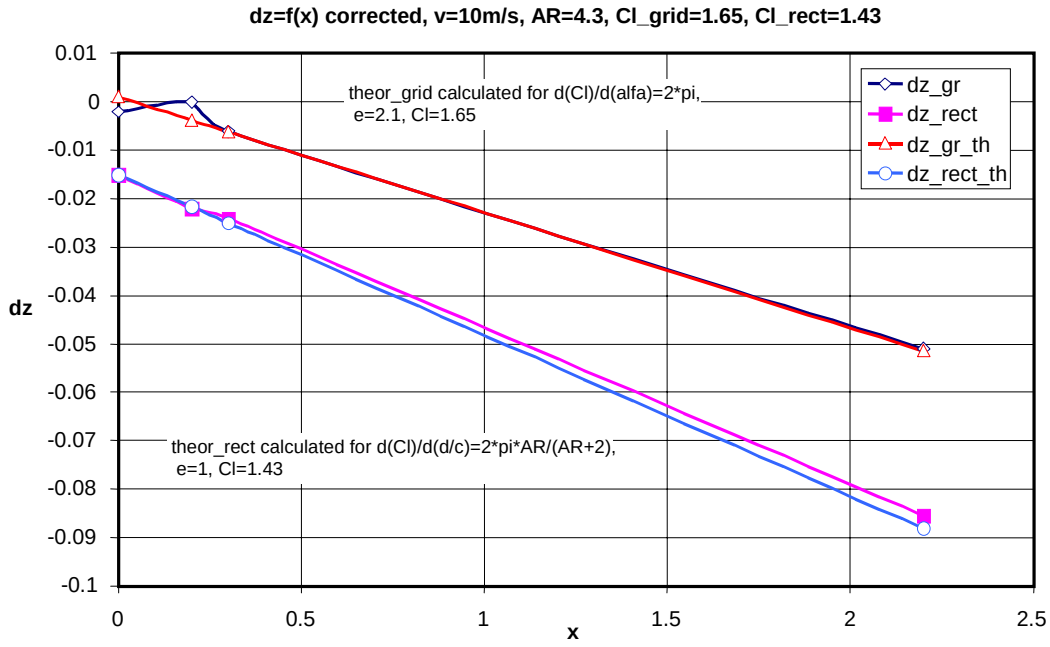

Figure 17: testdata PIV of vertical displacement of vortices compared to extension of Spreiter & Sacks.

The following sequence, cf. figures 18,19, shows the PIV images as obtained at TNF Johannes Keppler Unversity Linz, Austria at station 0.2m and 2.2m for *rect* and *grid* used for verification of Spreiter & Sacks vertical displacement comparison.

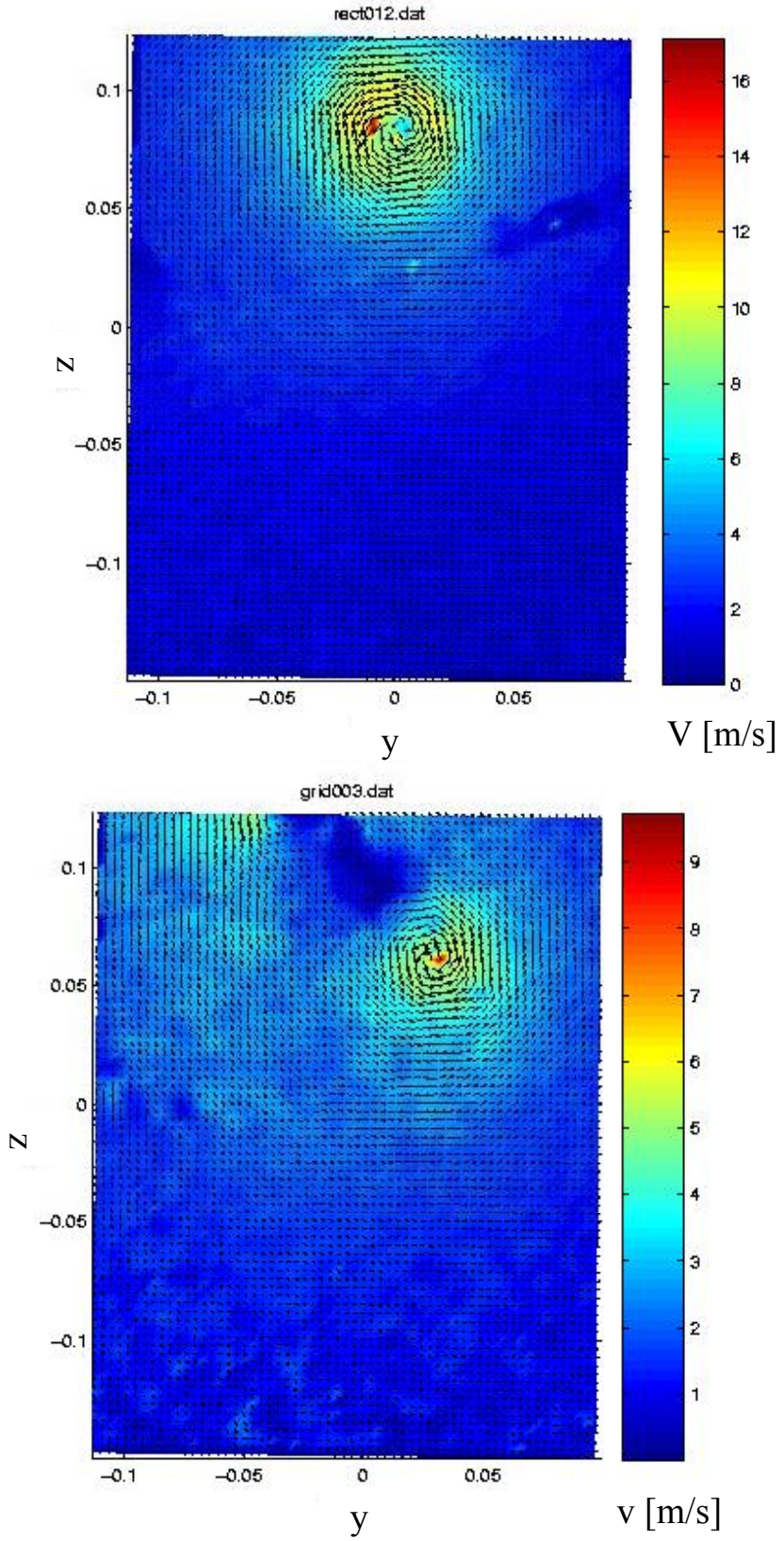

Figure 18: station 0.2m behind TE: top *rect*, bottom *grid* (vertical shear layer of Winggrid tip is just about folding into rolled up structure around dark still core), individual vortices of interference zone of blades with endplate visible, rollup structure of grid only starts to be defined. (in the idaflieg99 smoke visualisations this is about the station behind TE, where rollup of the vertical shear layer of the Winggrid tip is observed).

Note: In this and the next figure 19 the unit of coordinates y and z is [m]

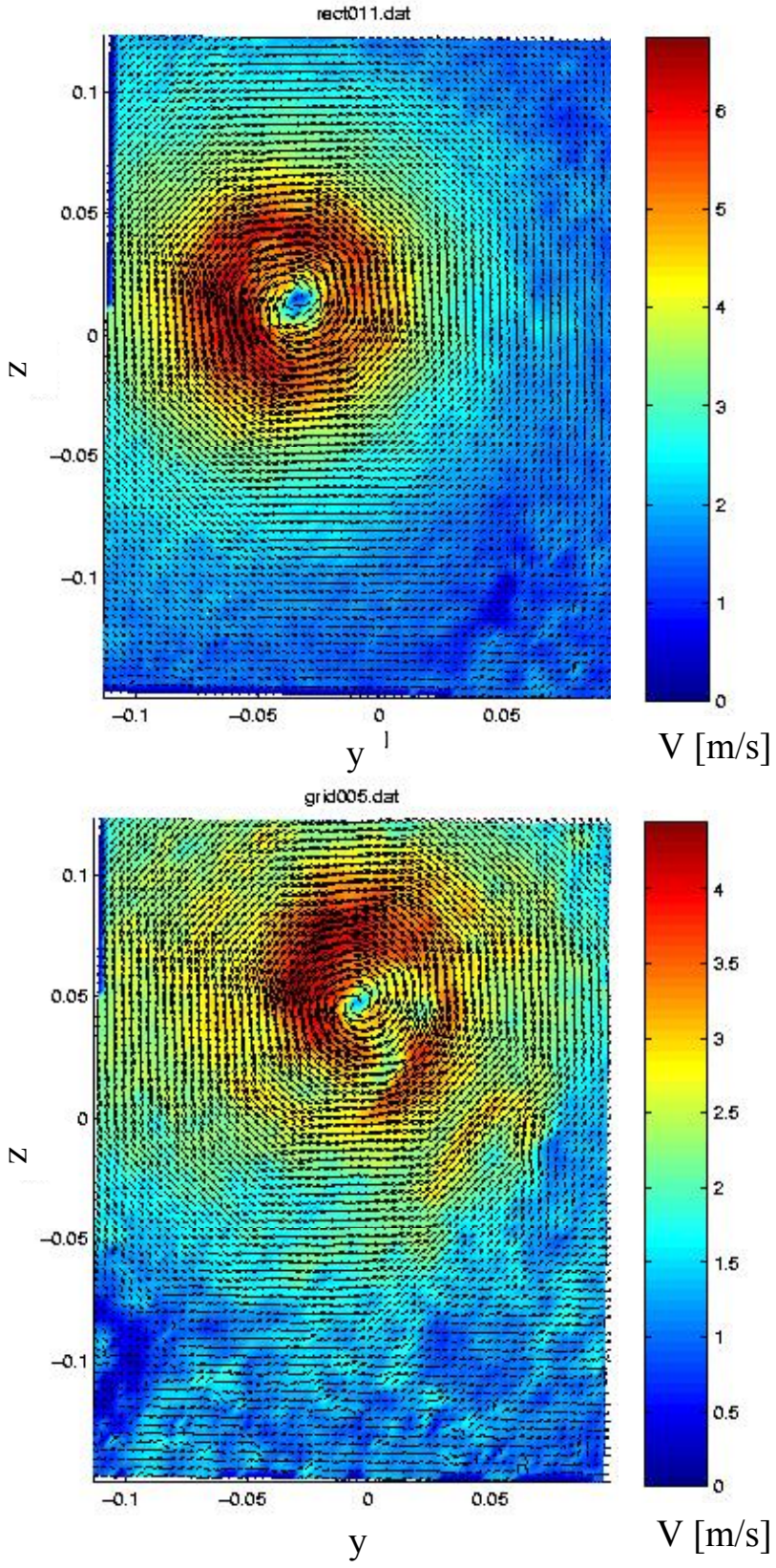

Figure 19: station 2.2m behind TE: top *rect* is displaced horizontal by further rollup, bottom *grid* is fully rolled up with neglible horizontal displacement compared to station 0.2m - vertical displacement less than *rect*.

F. Summary

We think PIV to represent a neat quantitative method for testing experimentally the span efficiency of a general wing system, independent of viscous drag present as long as there is no separation.

In the case reported, the results obtained are in acceptable agreement with:

- Polar measurements in control line model setup La Roche Consulting (identical wing with Winggrid tip and elliptic tip at respective Re number and Cl)
- Extended LINAIR PRO calculations using Betz grid approximation.
- Smoke visualisations with Biot-Savart reconstruction of vortex structure and rollup idaflieg99 fullscale tests

For the most general case with arbitrary span load and span efficiency the detailed expressions given by e.g. Spreiter & Sacks have to be used for calculating the vertical displacement speeds of the center of the wake and the centers of the vortex pair. We think that using measured separation of the c.g. of vorticity leaving the wing system in question would provide an experimental check of these calculations.

References

[1]Munk, Max M., "The Minimum Induced Drag of Aerofoils", NACA Report 121

[2]Procter, P., "Winglet designs to cut fuel burn", Aviation week & space technology, Dec 6, 1994, p.3

[3]Smith, S.C., "A Computational and Experimental Study of nonlinear Aspects of Induced Drag", NASA Technical Paper 3598, Ames Research Center, 1996

[4]La Roche, U. and Palffy, S.,"WING-GRID, a Novel Device for Reduction of Induced Drag on Wings", Proceedings ICAS 96 Sorrento (Italy), September 8-13, 1996, ISBN 1-56347-219-8

[5]LINAIR PRO, Version 3.4 for MS Windows, Desktop Aeronautics Inc. 1987, P.O. Box A-L, Stanford CA

[6]Spillman, John J. , US patent 4,272,043, 1981

[7]Spreiter, J.R.,and Sacks, A.H., "the rolling up of the trailing vortex sheet and its effect on the downwash behind wings", Journal of the Aeronautical Sciences Jan. 1951, p. 21 ff.

[8]Prandtl, L., "aerofoil lift and drag in theory", Jb. Wiss. Ges. Luftfahrt, vol V, 1920

[9]Cone, C.D., "The theory of induced lift and minimum induced drag of nonplanar lifting systems" , NACA technical report R-139 1962

[10]Kroo, I., "Drag Due to Lift: Concepts for Prediction and Reduction", Annu. Rev. Fluid Mech. 2001, pp. 587/617

[11]Oswatitsch, K., Gasdynamik, pp. 217, Springer 1952, Wien

[12]Betz, A., Gitterwirkungszahl, Hütte I, pp. 808, Wilhelm Ernst & Sohn, Berlin

[13]La Roche, U. and L.,"WING-GRID, Development, Qualification and Fligth Testing of a WINGGRID on a jetpowered testbed", Proceedings ICAS 98 Melbourne (Australia), September 13-18, 1998, AIAA

[14]La Roche, U. and L. ,"Induced Drag Reduction with the WINGGRID", Proceedings CEAS Potsdam 2000, European DragNet, NNFM 76, Springer, ISBN 3-540-41911-0

[15]idaflieg99, Berichtsheft XXVI – 2000, pp. 79, M. Wehle, Bonn 2001

[16]Betz, A.,"Behaviour of Vortex Systems", NACA TM 713, 1933